Defects Detection in PCB Images by Scanning Procedure, Flood-filling and Mathematical Comparison

ROMAN MELNYK, ANDRII SHPEK
Software Department,
Lviv Polytechnic National University,
12 Stepan Bandera St., Lviv, 79013,
UKRAINE

Abstract: - The basis of the approach is a scanning procedure with the movement of windows on the printed circuit board to detect defects of various types. Mathematical image comparison, pixel distribution histograms, padding algorithms, statistical calculations, and histogram deviation measurements are applied to the small parts of the PCB image in a small window area. The paper considers K-mean clustering of pixel intensities to simplify the printed circuit board image, separation of elements on the printed circuit board image by filling with colors, determination of defect intensity, and subtraction formulas.

Key-Words: - Scanning, printed circuit boards, chains, defects, clustering, flood-filling, pixel histogram, statistical features, greyscale, tolerance.

Received: February 13, 2023. Revised: November 22, 2023. Accepted: December 12, 2023. Published: December 31, 2023.

1 Introduction

Scanning methods are used in various scientific studies. The purpose of their research is to increase the amount and accuracy of data for designing and researching objects. As a rule, special devices based on lasers, ultrasound, and X-ray machines are used for scanning. The data is collected effectively via laser-scanning microscopy, or they are used for image-recognition algorithms in the context of post-fabrication defect detection, [1], [2]. Such devices and algorithms are inserted into powerful software classifying faults in different surface boards, [3], [4].

The main advantage of scanning is the relative increase in the area with the objects of attention due to the rejection of the prevailing other surroundings. That is why scanning is applied to problems of defect detection in printed circuit boards.

For inspection of inaccuracies in PCB production, neural networks are used and described in articles, [5], [6], [7], [8], [9]. Other works contain subtraction algorithms, [10], [11], [12]. The earlier article uses a table of connection traces based on contacts from the etalon image, [13]. Defects in traces and contacts of such types as shift, and extra metal are not analyzed.

The surveys contain many references in publications describing approaches and methods for the detection and classification of defects in printed circuit boards, [14], [15]. The main ideas of] subtraction of images, defects extraction, thinning, and increasing the visibility of elements on the board are considered in the works, [16], [17], [18]. The subtraction operations between PCB images are sensible to a deviation of the sizes of traces and contacts from the etalon. They give extra or lacking pixels that do not affect the correct operation of the electrical scheme.

Short, open circuits and depression changes in computer vision and artificial intelligence inspection systems are subjects in publications, [19], [20]. All mentioned approaches differ between themselves by complexity, input data, and characteristics of their implementation.

In this paper, the following approaches are applied to solving the problem: principles of scanning windows on the board, mathematical formulas of comparison, histograms of pixels from the OX and OY axes, the filling algorithm for dividing and selecting chains, the K-means clustering algorithm, formulas for calculating the statistical characteristics of circuit components.

The advantages of the proposed method are the detection of three classes of defects: connection, excess, and lack of metal on tracks and contacts. Areas with found defects are marked with colored zones directly in the places of their permanent location. This creates the possibility of additional analysis of suspicious areas of the installation for repairability or complete failure.

2 Determination of Defect Intensity

Some examples of PCB defects that often occur are shown in Figure 1. They are short, open, incorrect sizes, and various inaccuracies of contacts.

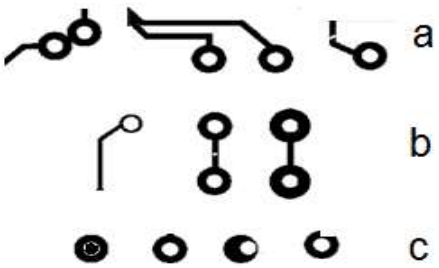

Fig. 1: Three types of defects: short and open (a), sizes and inner defects (b), extra or lacking metal (c)

Some of these types of defects are presented on manufactured PCB samples. An example of the PCB image with four defects is shown in Figure 2. They are marked by serial numbers. Open (4) and short (3) defects are made by very thin black and white lines of the one-pixel width. Two contacts (1,3) are deformed by a lack of metal.

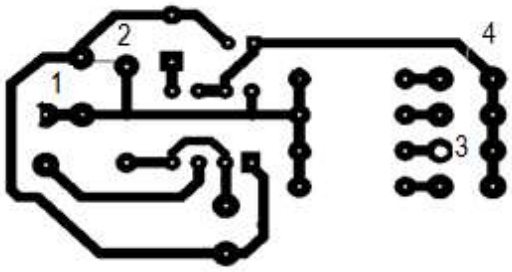

Fig. 2: PCB image with four defects

To measure these defects two histograms of pixels on the OX or OY axis are calculated for the reference and defective PCB images. The numbers of pixels in columns or rows are calculated for the interval of intensity $I(\text{int})=0\div10$ as follows in the formulas:

$$h(c)=card\{(x,y)\big|I(x,y)\subset I(\text{int})\},$$
$$h(r)=card\{(x,y)\big|I(x,y)\subset I(\text{int})\},$$
$$(c=0,1,...,w;\ \ r=0,1,...,H).$$

An example of defects affecting the quantitative histogram function in a column is demonstrated by the graphs in Figure 3. The graphs are calculated for reference and defective PCB images in the intensity $0\div10$ interval. Only two very small differences mark defects 3 and 4. The contribution to the graph from all four defects is very small. For the row function, the difference is even smaller.

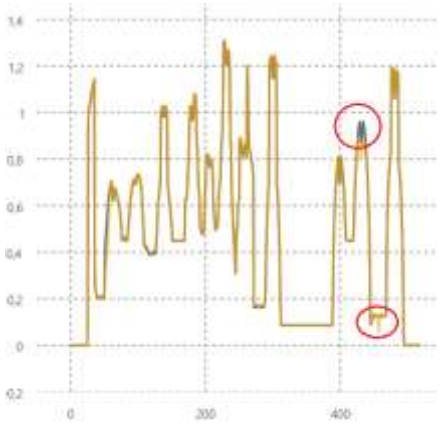

Fig. 3: Two histograms of black pixels in two PCB images along the OX axis

The reason is that the number of pixels reflecting defects is very small compared to the number of white or black pixels of the whole image. Even having the reference image, they are superimposed on the inaccuracies of manufacturing PCBs.

The opposite case is observed when only two chains or their fragments are measured by the number of pixels. Examples of the two fragments and their histograms along the OY axis are shown in Figure 4. Values differ by 20-40 percent due to the location of the defect and by 2-4 percent due to different widths of traces.

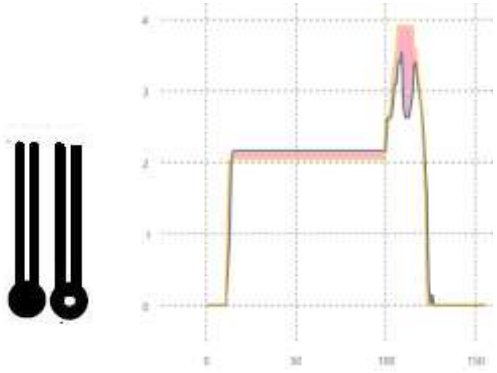

a b

Fig. 4: PCB fragments (a) and histograms of black pixels along the OY axis (b)

3 Comparison Formulas for Detection and Separation of Defects

Traditionally, defects in the PCB image are detected by XORing the binary images. The XOR operations with pixels are as follows:

$$0 \wedge 1 = 1, 1 \wedge 0 = 1, 0 \wedge 0 = 0, 1 \wedge 1 = 0,$$

where 0 denotes white and 1 denotes black or vice versa.

These operations show the inaccuracies and defects of the manufactured printed circuit board about the reference sample. Surpluses and shortages of metal on tracks and contacts belong to one class.

To separate positive and negative defects, subtraction operations are applied to the binary images:

$$0 - 1 = 0, 1 - 0 = 1, 0 - 0 = 0, \ 1 - 1 = 0.$$

Such operations are repeated twice: until a positive and negative result is obtained. Different results are achieved by exchanging the input images after the first subtraction. The resulting images contain white areas and lines representing various types of defects. Two examples of result images from [8], are shown in Figure 5. Two input binary PCB images are not shown because only results are presented for comparison with the below-following approach.

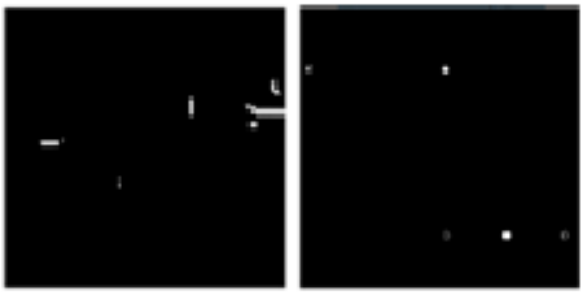

Fig. 5: Images after subtraction of binary PCB images

The results obtained are not good enough in terms of the location, size, and intensity of the white figures. The main drawback is their separation from the elements of the scheme. It is a significant problem, especially for the printed circuit boards of large sizes.

That is why a new approach has been developed to increase the visibility of defective pixels. It is used for their separation, determination of coordinates, visual inspection of defects, and future application of neural networks. The separation is both from structural elements and between classes with excess and shortage of metal.

When two images are compared, they are input data for the following comparison formulas:

$$I_r(x,y) = I_d(x,y) \quad \forall |I_e(x,y) - I_d(x,y)| < Tol,$$

$$I_r(x,y) = RGB(|I_e(x,y) - I_d(x,y)|,00),(red)$$
$$\forall |I_e(x,y) - I_d(x,y)| \geq Tol,$$

and a sign is +,

$$I_r(x,y) = RGB(0,|I_e(x,y) - I_d(x,y)|,0),(blue)$$
$$\forall I_d(x,y) - I_e(x,y) \geq Tol \ ,$$ and a sign is -,

where $I_r(x,y)$ is the pixel intensity of the resulting image, $I_e(x,y)$ is the pixel intensity of the first image, $I_d(x,y)$ is the pixel intensity of the second image, Tol is the tolerance value for controlling the difference between the pixel intensity of the etalon and controlled sample.

The comparison formula is applied to the etalon and the PCB image with four defects. The marked defects with blue and red in the difference between them are shown in Figure 6. The short defect is blue, and the shortage of metal is marked with red (including the open defect).

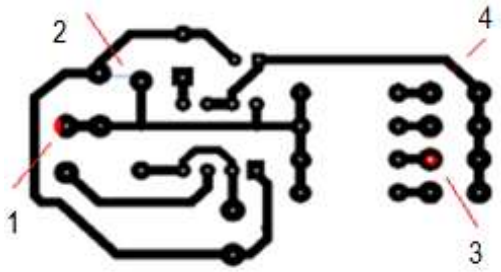

Fig. 6: Difference image with four marked defects

Every type of defect has its color (intensity). Thus, for them, a histogram of pixels on the OX or OY axis is applied. The colors (blue and red) are of 29 and 79 intensities. So, for these points of intensity from the interval 29-79, the numbers of blue and red pixels in columns are calculated and shown in Figure 6.

The number of blue pixels is small about the number of red pixels. The histogram reflects the relative numbers of pixels. That is why values for blue pixels are small. It is convenient to use the cumulative histogram for calculations:

$$H_i(c) = \sum_{k=1}^{i} h_k(c), H_i(r) = \sum_{k=1}^{i} h_k(r),$$
$$c = 1,2,...W, r = 1,2,..., H,$$

The cumulative histogram together with its piecewise linear approximation is shown in Figure 8.

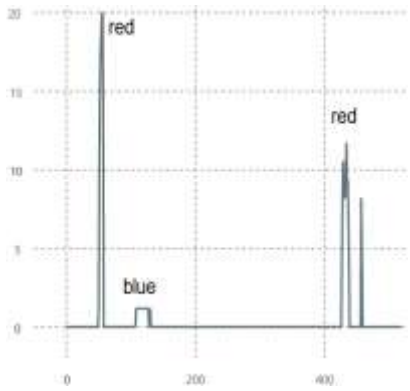

Fig. 7: Histogram of blue and red pixels in PCB image by the *OX* axis

When approximating the cumulative histogram by the piecewise linear function the obtained points in Figure 8 indicate the amount of red and blue pixels. Concretely, a vertical difference of the ordinate values gives the relative number of pixels with a defined OX coordinate.

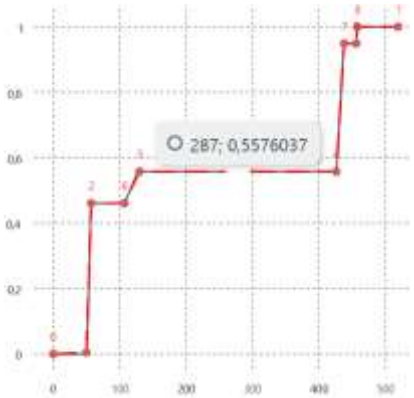

Fig. 8: Cumulative histogram and its approximation of red and blue pixels in PCB image by the *OX* axis

There are four groups of pixels having the following numbers:

$$N_1 = H(2) - H(1), N_2 = H(5) - H(6),$$
$$N_3 = H(3) - H(4), N_4 = H(8) - H(7),$$

where N_1,.. and N_4 are amounts of red and blue pixels distributed within the coordinates on the OX axis.

When three graphs built by their scales are presented in one field the axis OY reflects only the maximal interval of one graph and shows the relative values. They are different in the different measurements. It is demonstrated in Figure 9.

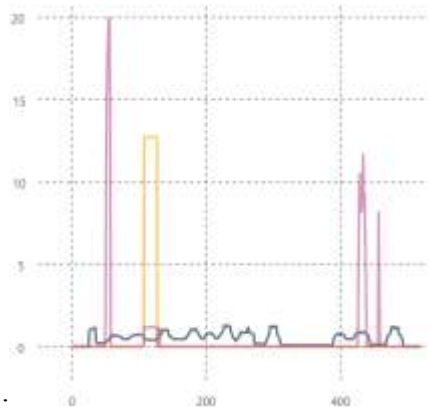

;

Fig. 9: Three histograms in PCB image along the *OX* axis: for black (grey), blue (yellow), and red (violet) pixels

The experiment confirms that for the separation of pixels, different histograms are needed to measure different types of defects. In both cases, the actual number of blue and red pixels is considered. This number is calculated from cumulative histograms or by the following formulas:

$$N(red) = S(r) * \sum_{1=1}^{Nc} K_i(r), N(blue) = S(s) * \sum_{1=1}^{Nc} K_i(s),$$

where $S(r), S(s)$ are the numbers of pixels in the whole etalon and sample images, $K_i(r), K_i(s)$ are the relative numbers of pixels in one column, N_c is the number of columns containing red (blue) pixels.

The interval must be indicated because error values are very small, and the number of black pixels is very large.

They are also very small for the interval as this is shown in Figure 2 where absent pixels in defective places are almost invisible. There is one way to increase the visibility of pixels indicating blue and red pixels of defects. The relative weight of defective pixels must be increased, and the relative weight of surrounding pixels must be decreased. It can be reached by decreasing the area for measurement. One of the possible approaches is to measure consequently quantitative characteristics of parts of the PCB image to be compared by the scanning procedure.

4 Scanning Procedure

In the scanning process, two input images are covered with the same grid at the step of the user. The image with marked defects covered with a 5x3 grid is shown in Figure 10.

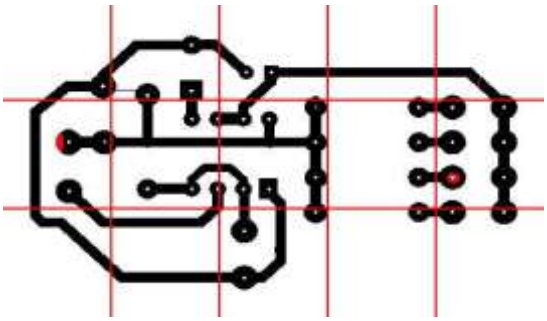

Fig. 10: Defective PCB image covered by 15 cell-windows

Then all corresponding pairs of rectangles in the input and defective PCB images are compared by one of the developed approaches. For the 5x3 grid such operations are repeated 15 times.

To reduce the influence of the positions of the grid lines on the results of calculation the PCB image is covered by a sequence of rectangles with intersecting areas. The sequence is built when the rectangle window scans the surface of the image. Then informative pixels are included into rectangles two times. Figure 11 shows two not intersected and two intersected windows: in the first case, the second window does not contain the defect together with the contact, the second window contains them. The intersected area is marked with an orange color.

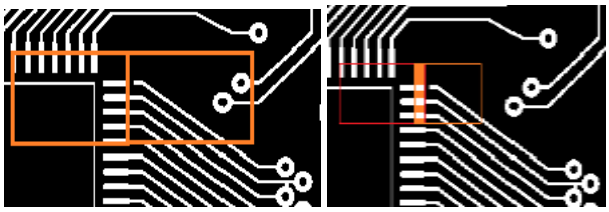

a b

Fig. 11: Two windows of different sizes in the image: not intersected (a), intersected (b)

The comparison procedure repeats its work step by step covering the whole image area in a sequence of the smaller areas. Intersection occurs on the right (left) and down (top) borders of the scanning rectangle (Figure 12). Twice intersected areas are marked with a pink color. Areas belonging to four scanning windows are marked with a red color. Only four scanning windows are shown in Figure 12.

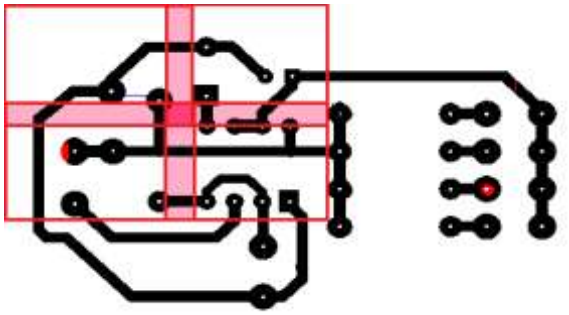

Fig. 12: Four scanning windows on the board

Every window is analyzed as being fully independent. Previous and subsequent data are not considered. The sizes of windows and intersections are set by the user given the need for accuracy and time consumption.

Examples of three fragments with defects are shown in Figure 13. These fragments are input data for scanning windows. Defects are marked with red and blue colors.

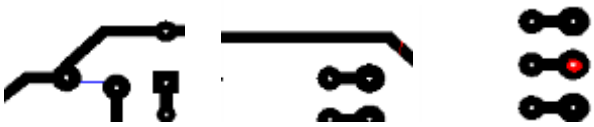

a b c

Fig. 13: Three fragments with defects: short (a), open (b), and lack of metal (c)

Measurement of defects is made by calculation of two histograms like those given in Figure 7. Histograms are data for the determination of the numbers of blue and red pixels separately according to their intensity:

$$h(c) = card\{(x,y)|I(x,y) \subset I(int)\},\text{cr}$$

$$h(r) = card\{(x,y)|I(x,y) \subset I(int)\},$$

$$(c = 0,1,\dots,w; r = 0,1,\dots,H).$$

$$I(int) = blue, I(int) = red.$$

The criterion function is built to check possible defects of any type in the examined fragment of the printed circuit board in the window according to the formulas:

$$D_f(w) = \{\sum |H_r(i) - H_s(i)|, i = 1,2....,w;$$
$$D_s = sort\{D_f, D_f > tol\}$$

where $H_r(i), H_s(i)$ are the histogram values of the reference and sample images in the window,

D_s, D_f are the function values in sorted and unsorted arrays, and *tol* is the tolerance value to control the intensity of marked inaccuracies on the board.

After the scanning process is completed, all windows are characterized by the coordinates and values of the criterion function stored in the array D_s. The array is sorted in ascending order. Windows with features exceeding the tolerance are superimposed on the red or blue image. The color depends on the type of defect: lack of metal on the board with a red rectangle, excess metal on the board with a blue rectangle. An overlay is realized by the following formula applied to every channel of the pixel:

$$I_r(x,y) = \alpha I_c(x_i, y_i) + (1-\alpha) I_b(x_i, y_i)_i(r),$$

where I_r, I_c, I_b are the pixel intensity of the resulting, colored, and printed board images, α is the coefficient of transparency.

Scanning the defective image in Figure 2 reveals all four defects that were not present in the PCB reference image. The result is shown in Figure 14.

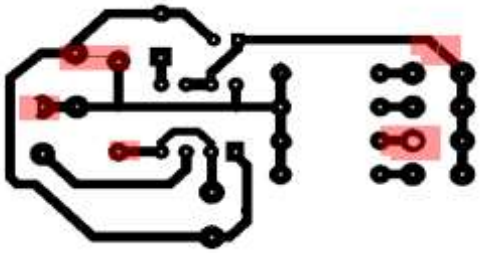

Fig. 14: Four places with defects after scanning

The red rectangles of different intensities contain the locations of four defects: open, short, and metal-free in the contacts. The intensity of blue and red colors is proportional to the value of the criterion. The types of defects are not defined.

5 Connection Defects Detection

The scan detects defect locations and visually illustrates their intensity. But that doesn't answer the question “Is there a connection defect? And if so, what type? The following approach provides such an answer.

A flood-filling algorithm is used to separate and compare connected circuits on the reference and fabricated PCB images with short and open defects. For example, they are marked with different colors and shown in Figure 15 and Figure 16. Four histograms for them are calculated and shown in Figure 17 and Figure 18.

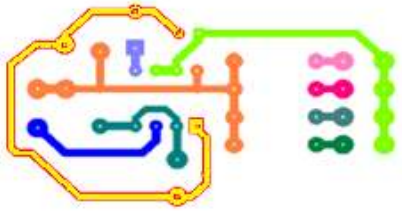

Fig. 15: Input flood-filled image

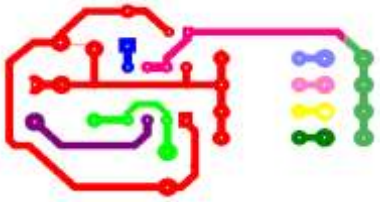

Fig. 16: Flood-filled image with defects

The two filled images contain the same components with different colors. The reason is that the second image contains open and short defects that provoke changes in the distribution of pixels. The second reason is that a special procedure is needed to find the starting points belonging to the same chains on both PCB images.

To detect connection defects, it does not matter what colors the circuits are filled with.

As a rule, if the number of components is different, there is a connection defect in the circuit. Sometimes two defects can be observed if the number of components is the same as in the input image. In this case, an open defect is compensated by a short defect.

Calculation of the number of pixels in all circuits of the input image of the printed circuit board gives the following distribution (in percentages) of the components: 0.5 (5), 1.4 (2), 3.4, 3.5, 4.8. This distribution is related to the total number of pixels in the image. It is calculated by traversing the pixels of the image matrix to form the ordinary and cumulative histograms.

The image of the defective printed circuit board gives the following distribution (in percentages) of the components: seven as in the reference image 0.5 (5), 1.4 (2), and three as the new components 1.6, 1.8, 8.4. The new values 1.6 and 1.8 correspond to the broken chain 3.4. The combined chains 3.5, and 4.8 correspond to the value 8.4. Thus, three new components were created.

This fact is illustrated by the two cumulative histograms in Figure 17. The blue histogram belongs to the input image and the red histogram represents the defective image. Each histogram has

ten steps representing ten components. The step's height corresponds to the number of pixels. The OX coordinates indicate the intensity values of the components. Two histograms do not coincide due to the different colors of the same components in two images, and three different components.

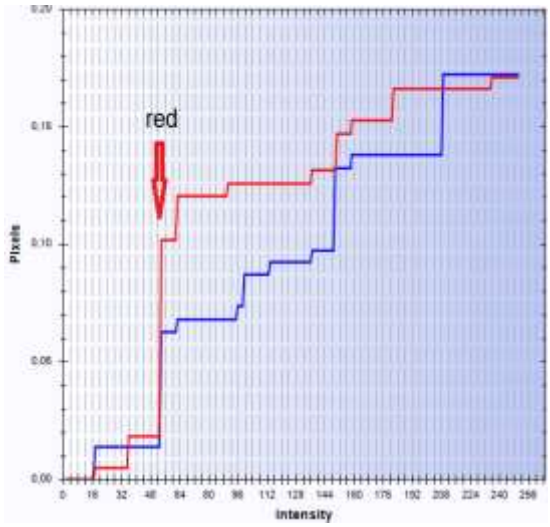

Fig. 17: Cumulative histograms of two flood-filled images: input (blue) and with defects (red)

The component distributions found are the basis for detecting connection defects. Among other methods, simply comparing elements from two arrays and eliminating similar components answers two questions: Are there any connectivity defects in the region? And "What circuits cause these defects?"

Each component has its identification number and color. The colors selected in the fill algorithm do not affect the number of steps in the cumulative histogram but only change their distribution on the OX (intensity) axis. The main requirement is that they be different. That way, when found, they can be selected and showcased.

To illustrate how colors change the pitch distribution, two cumulative histograms are calculated only for the reference PCB image. But once components are with one set of colors and then they are redrawn into the second set of other colors. The first histogram is marked in red and the second in blue, and they are shown in Figure 18. The coordinates of the steps do not coincide.

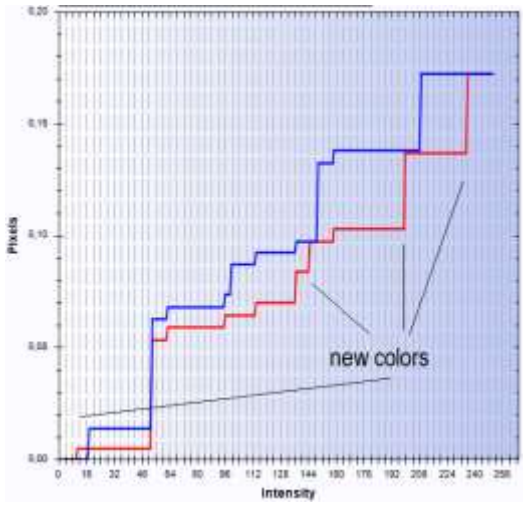

Fig. 18: Cumulative histograms of two flood-filled images: input (blue) and input with other colors (red)

Each window represents a cropped part of the printed circuit board image in the scanning process. Three examples with different defects are fragments of the entire PCB image. Using the filling algorithm, the black components of these parts are redrawn with different colors, and shown in Figure 19.

Fig. 19: Three fragments with defects: short (a), open (b), and lack of metal (c)

Calculation of the number of pixels in all circuits of the input image of the printed circuit board gives the following distribution (in percentages) of the components: Figure 11a) for the standard 0.034, 0.116, 0.04; for sample 0.04, 0.150; Figure 11b) for the standard 0.042, 0.071, 0.030; for the sample 0.007, 0.065, 0.029, 0.042; Figure 11c) for the standard 0.062, 0.062, 0.062; for the sample 0.056, 0.061, 0.061.

The number of components in the sample is changed: reduced to two instead of three in the reference image (Figure 19a) and increased to four instead of three in the image (Figure 19b). In the first case, there is a short defect and in the second - an open one. In Figure 19c no connection defect. Only the lack of metal is captured by quantitative analysis, which is detected and measured in the previous approach.

Mathematically, the problem is solved in two ways. In the first, the average size (number of

pixels) in one window is calculated using the following formulas:

$$S_j = card\{(x,y), I(x,y) = C_j\},$$

$$\bar{S} = 1/N_c \sum S_j, j = 1,2,..., N_c,$$

where $I(x,y)$ is the intensity of pixels in the j-th component with its color, C_j is the color of the j-th component, N_c is the number of components.

The variance or mean standard deviation of the calculated function is used to estimate changes in the component sizes in each window:

$$E^2(\mathrm{w}) = (1/N_c) \cdot \sum_{i=1}^{N} (S_i(w) - \bar{S}(w))^2,$$

where $\bar{S}(w)$ *is* the mean size of components in the w-th window, $S_i(w)$ is the size of the i-th component in the w-th window, $E^2(\mathrm{a})$ is the variance value of the corresponding window, $E\ (w)$ is the standard deviation.

For the above-described examples, these parameters are as follows.

1) The reference images:

$\bar{S}(a)$=0.063, $E^2(\mathrm{a})$=0.001393, $E(a)$ =0.037.

$\bar{S}(b)$=0.047, $E^2(\mathrm{b})$=0.000281, $E\ (b)$=0.017.

$\bar{S}(c)$=0.062, $E^2(c)$=0.0, $E\ (c)$=0.0.

2) The sample images:

$E^2(\mathrm{a})$=0.003025, $E\ (\mathrm{a})$ =0.055.

$E^2(\mathrm{b})$=0.000464, $E\ (\mathrm{b})$ =0.022.

$E^2(c)$=0.000006, $E\ (\mathrm{c})$ =0.002.

The first two variances of the controlled PCB images are larger than the etalon. In the latter case, the deviation changes are significantly smaller than in previous experiments due to a very small defect of the contact.

In conclusion, open and short defects cause the component size variance to change its value. The tolerance value divides these changes into two classes: insignificant due to inaccuracies and significant due to connection defects.

The second approach is also simple and accurate. It requires some mathematical calculations.

The components of the printed circuit board image contain many pixels, which are characterized by various distributed features. Among them, the average coordinates of the component are as follows:

$$\bar{x}(s) = 1/k_s \sum X(s),\ \bar{y}(s) = 1/k_s \sum Y(s),$$

$$x_i \in X(s), y_i \in Y(s)$$

where s is the component number, X, Y are sets of the pixel coordinates.

To obtain a parametric feature associated with pixel coordinates, the surface of the pattern is divided by a grid with steps along the OX and OY coordinates as shown in Figure 20. The grid cells are numbered as 1, 2, …, L_x*L_y from left to right and down from the top of the grid, where L_x, L_y are the column and row numbers on the OX and OY axes.

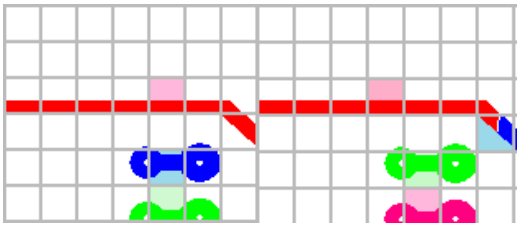

a b

Fig. 20: Two PCB fragments covered by a grid: without defects (a), open defect (b),

The grid step is selected as a tolerance value when comparing two windows containing the reference part of the PCB image and the part of the controlled PCB image.

Each pixel with the average coordinates $\bar{x}(s)$, $\bar{y}(s)$ is associated with the cell number C_n and its coordinates by the corresponding formulas:

$$i = (\bar{x}(s)/L_x)_{ceil} + 1,\ \ j = (\bar{y}(s)/L_y)_{ceil} + 1.$$

$$C_n = (i-1) * L_x + j$$

For images in Figure 20 characteristics of cell numbers are represented by two diagrams in Figure 21. Two coordinate axes are the cell number 0÷C_n and the intensity interval 0÷255.

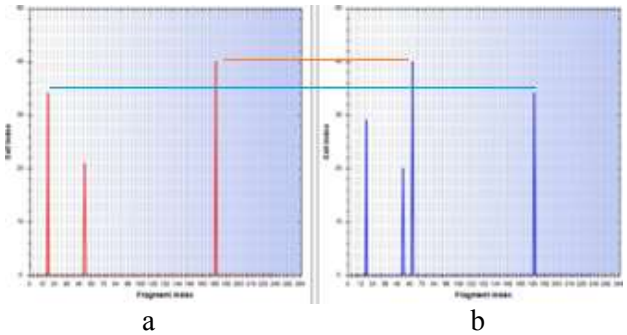

a b

Fig. 21: Number of cells containing average coordinates of components: etalon image (a), sample image (b)

In Figure 21a the cell ordinates are 19, 33, and 40. In Figure 21b, the four ordinates of the cells are 18, 28, 33, and 40. All these cells are marked with

colors in the corresponding grids in Figure 20. On both diagrams in Figure 21 the identical ordinates are indicated by two parallel lines. Thus, one component of the reference image is split into two components. The conclusion is made that an open defect is in the current window.

The final function of the criterion is built from the two components: the difference in the variances of the component sizes on the two parts of the different boards and the difference between the cell numbers with the average coordinates of the components of the two boards. It is built to check for possible existing connection defects in the examined fragment of the printed circuit board according to the formula:

$$F = \{w_1 \left| E^2{}_r - E^2{}_s \right| + w_2 \sum_{1=1}^{K} \left| C_{ni}(r) - C_{ni}(s) \right| < tol \quad ,$$

where $C_{ni}(i_r, j_r)$ $C_{ni}(i_s, j_s)$ are the numbers of the rows and columns of the two cells containing the average coordinates of components, $E^2{}_r, E^2{}_s$ are the variances of the component sizes, w_1, w_2, are the weighting factors. Summing up takes place by all components; K is their number.

The weighting factors play an important role because the order of values in the two terms is different. When the second term is nonzero, the monitored sample has a new component, or some component is shifted. At the end of the procedure, this part of the PCB image is marked as defective.

6 Full Colored Images

An example of the printed circuit board image with two defects (broken and short) is shown in Figure 22. The image has three main colors: a dark green background, green traces, and yellow contacts.

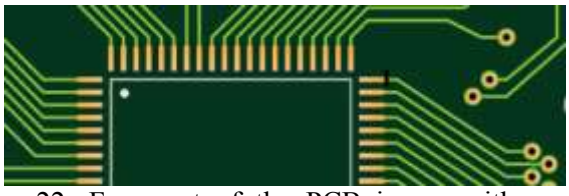

Fig. 22: Fragment of the PCB image with green routes and yellow contacts

Mathematical formulas are calculated to compare both images: the original in full color and grayscale to detect the pixels that mark defects. The results are shown in Figure 23. The number of red and blue pixels is very small in each image, and it does not affect the calculated function based on the pixel intensity.

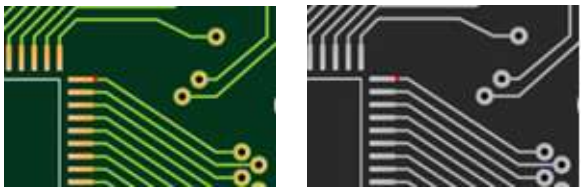

a b

Fig. 23: Fragments of image difference: full color (a), grey gradations (b)

It is also difficult to separate these pixels because their intensity values are the same as the intensity values of the surrounding pixels according to the interval 0÷255. Examples are shown in Figure 24.

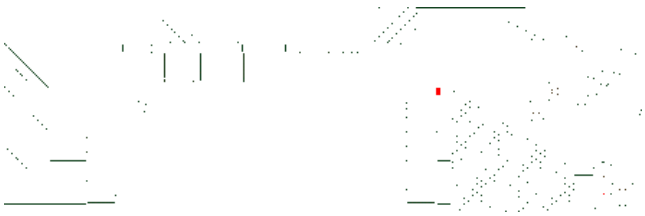

Fig. 24: Intensity levels containing red and blue pixels

Better results are achieved when the greyscale image is clustered. Pixels in clusters have the same color, and pixels of other colors are easy to separate. Figure 25 shows three and two groups of pixels in K=3 and K =2 cluster images. The first image contains three groups of pixels: contacts, traces, and backgrounds. The second image contains the background and the chains with the contacts.

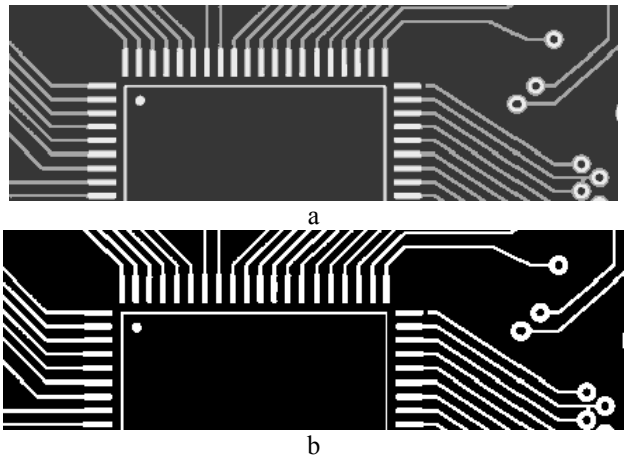

a

b

Fig. 25: Fragments of the defective PCB image: three clusters (a), two clusters (b)

Then mathematical formulas of the comparison are applied to the clustered images: the etalon and sample. Fragments after their logical subtraction are shown in Figure 26. The blue area is very small.

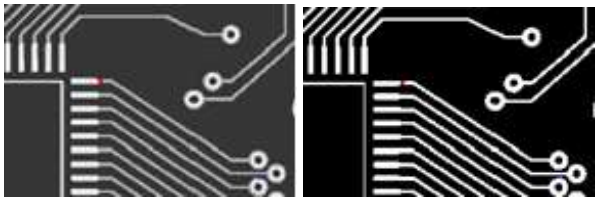

a b

Fig. 26: Fragments after comparison of the etalon PCB image with the sample image: three clusters (a), two clusters (b)

Red and blue pixels indicate open and short defects in the full-color and grayscale images. They are very small and almost invisible. However, they are easy to separate and calculate because their intensity values are significantly different from those of all other objects on the board. Examples of histograms for the number of red and blue pixels in columns are shown in Figure 27.

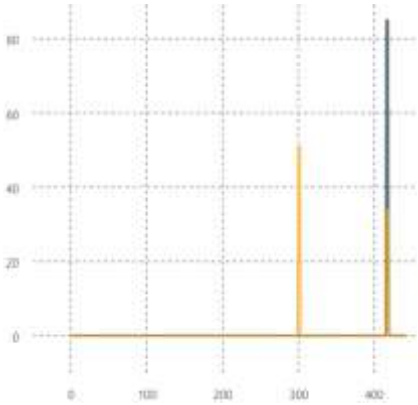

Fig. 27: Histograms of blue (blue) and red pixels (yellow)

These histograms are characteristics of the scan window. They are the input data to calculate the total number of red or blue pixels in the window:

$$N(red) = S(r) * \sum_{1=1}^{Nc} K_i(r), N(blue) = S(s) * \sum_{1=1}^{Nc} K_i(s),$$

where $S(r), S(s)$ are the numbers of pixels in the entire etalon and sample images, $K_i(r), K_i(s)$ are the relative numbers of pixels in one column, N_c is the number of columns containing red (blue) pixels.

In addition, the clustered images are suitable for finding connectivity defects, since the colors of the board objects are uniform, and suitable for filling algorithms.

One feature of clustered images should be considered. For the three formed clusters, contacts and traces are separate objects. With two clusters, contacts in combination with traces are considered as one object. When applying the filling algorithm, the first case is shown in Figure 28a, and the second in Figure 28b.

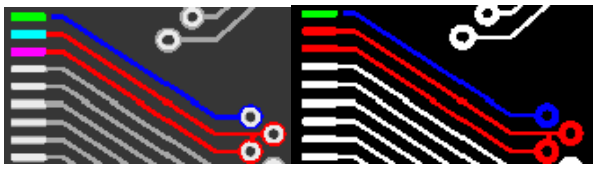

a b

Fig. 28: Filling in fragments of PCB image: three clusters (a), two clusters (b)

In the case of three clusters, the lack of metal cannot be classified as a connection defect because it is between components of different colors. From this point of view, two clusters in the image are a simpler and more reliable mechanism for further processing.

7 Experiments

Three approaches are realized for testing and comparing their effectiveness. They are 1) calculation of two histograms for the etalon and sample PCB images, 2) calculation of one histogram for red and blue pixels obtained from the mathematical comparison of the input images, 3) calculation of statistical features (variance and average coordinates) for components in two windows.

The developed algorithms are tested on different types of images. Three images of the following dimensions 440x140, 650x480, and 740x640 are input data for the developed software. Two clustered greyscale and one full-color image were taken for the experiments. In all cases, open and short defects are detected by scanning with nearly 1500 windows. The results are shown in Figure 29.

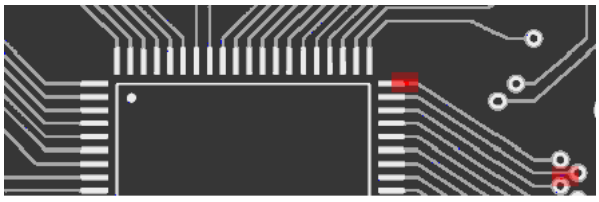

a

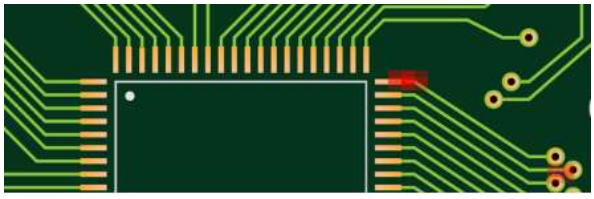

b

Fig. 29: PCB images after scanning: greyscale (a), full color (b)

The next PCB image has contacts of a grey color, and the board surface is fully covered by conducting metal (Figure 30). One contact is defective. The dimension of the scanning window is 30x20 with a cross-section of 10 along the OX axis and 5 along the OY axis. Nearly 6000 windows were analyzed with these initial conditions.

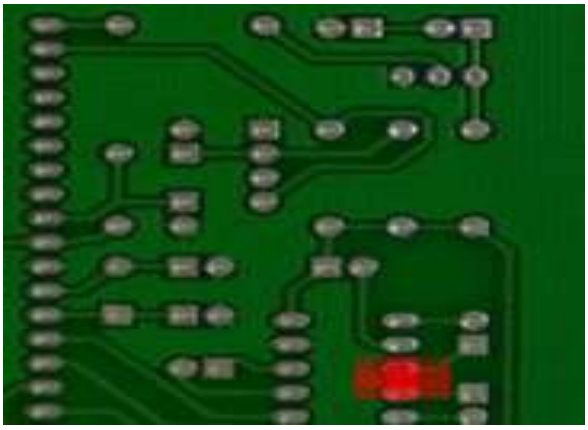

Fig. 30: PCB image after scanning

The third experiment is with the largest full-color PCB image shown in Figure 31. It has two defective contacts with extra metal. More than 7000 windows were analyzed to find and mark areas containing contacts with defects.

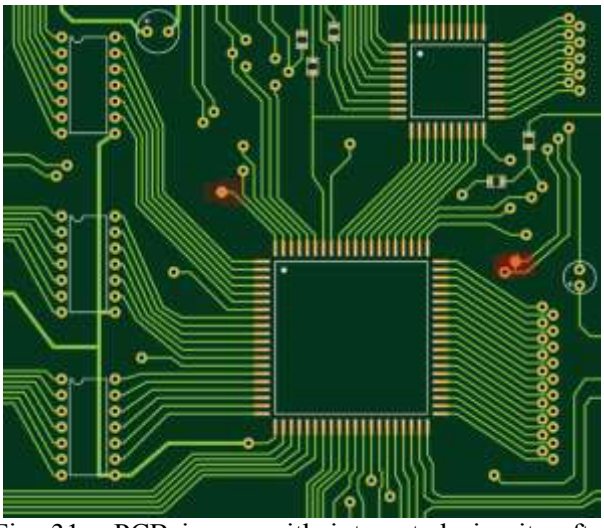

Fig. 31: PCB image with integrated circuits after scanning

All image transformations, calculations of functions, and formulas are implemented in the developed software and are invisible to the user. The engineer controls the window sizes, the tolerance values, and the method to be used in the analysis.

8 Conclusion

The approach is based on a scanning procedure in which the analysis of the entire large image is replaced by many analyses in much smaller areas of the printed circuit board. The analysis includes such approaches and methods as mathematical formulas of comparison, histograms of pixels from the OX and OY axes, the filling algorithm for dividing chains, the K-means clustering algorithm, and formulas for calculating the statistical characteristics of circuit components.

The proposed approach contains operations for the selection of three classes of defects: negative, positive, and connection. Marked with different colors, these defects are designed to train neural networks with different architectures for further automatic detection of defects and their classification. Together with the developed software, they will also indicate their locations and determine their intensity. In total, such software will reduce the hardware and make the PCB diagnostic process cheaper.

References:

[1] Sayed Hoseini, Gaoyuan Zhang, Alexander Jo ngbloed, Christian Schmitz, Christoph Quix, Automated defect detection for coatings via height profiles obtained by laser-scanning microscopy, *Machine Learning with Applications,* Vol. 10, December 2022, 100413.

[2] S. Zhang, Z. Chen, K. Granland, Y. Tang ,C. Chen, Machine Vision-Based Scanning Strategy for Defect Detection in Post-Additive Manufacturing, *NICOM 2022: Nanotechnology in Construction for Circular Economy, Lecture Notes in Civil Engineering book series (LNCE),* Vol. 356, pp. 271–284.

[3] Zahia Guezoui, Aicha Baya Goumeidane, Nafaa Nacereddine, Weld Defect Radiographic Image Segmentation with Finite Mixture Model (FMM), *Engineering World*, 2020, Vol. 2, pp. 134-138.

[4] Stella Vetova, Covid Image Classification using Wavelet Feature Vectors and NN, *Engineering World*, 2021, Vol. 3, pp. 38-42.

[5] Cai L., Li J., PCB defect detection system based on image processing, *Journal of Physics: Conference Series*, 2022, Vol. 2383, No. 1. pp. 012077.

[6] S. McClure. Extracting and Classifying Circuit Board Defects using Image Processing and Deep Learning, Feb. 4, 2020, [Online].

https://towardsdatascience.com/building-an-end-to-end-deep-learning-defect-classifier-application-for-printed-circuit-board-pcb-6361b3a76232, (Accessed Date: February 1, 2024).

[7] V. A. Adibhatla, H.-C. Chih, C.-C. Hsu, J. Cheng, M. F. Abbod, and J.-S. Shieh, Defect Detection in Printed Circuit Boards Using You-Only-Look-Once Convolutional Neural Networks, *Electronics*, Vol.9, No.9, 2020, pp. 1547.

[8] Abhiroop Bhattacharya, Sylvain G. Cloutier, End-to-end deep learning framework for printed circuit board manufacturing defect classification, *Scientific Reports*,2022, [Online]. https://www.nature.com/articles/s41598-022-16302-3, (Accessed Date: February 1, 2024).

[9] Jungsuk Kim, Jungbeom Ko, Hojong Choi and Hyunchul Kim, Printed Circuit Board Defect Detection Using Deep Learning via A Skip-Connected Convolutional Autoencoder, *Sensors*, No.21(15), 2021, 4968.

[10] Zhu, A. Wu and X. Liu, Printed circuit board defect visual detection based on wavelet denoising, *IOP Conference Series: Materials Science and Engineering*, Vol. 392, 2018, pp. 062055.

[11] Y. Hanlin and W. Jun, Automatic Detection Method of Circuit Boards Defect Based on Partition Enhanced Matching, *Information Technology Journal*, Vol.12, No.11, 2013, pp. 2256-2260.

[12] Vikas Chaudhary, Ishan R. Dave and Kishor P. Upla, S. V., Visual Inspection of Printed Circuit Board for Defect Detection and Classification. *International Conference on Wireless Communications, Signal Processing and Networking (WiSPNET)*, 2017, pp. 732-737.

[13] M. H.Tatibana, R. and de A. Lotufo. Novel Automatic PCB Inspection Technique Based on Connectivity, *Proceedings X Brazilian Symposium on Computer Graphics and Image Processing*, 1997, pp. 187-194.

[14] K. P. Anoop, N.S. Sarath and V. V. Sasi Kumar, Review of PCB Defect Detection Using Image Processing, *International Journal of Engineering and Innovative technology (IJEIT)*, Vol.4, Is.11, 2015, ISSN: 2277-3754.

[15] D.B. Anitha, and M. Rao, A survey on Defect Detection in Bare PCB and Assembled PCB using Image Processing Techniques, *International Conference on Wireless Communications, Signal Processing and Networking*, 2017, pp. 39-43.

[16] M. Moganti, F. Ercal, C. H .Dagli, and S. Tzumekawa, Automatic PCB inspection algorithms: A review, *Computer Vision and Image Understanding*, Vol. 63, No. 2, 1996, pp. 287-313.

[17] F. B. Nadaf and V. S. Kolkure, Detection of Bare PCB Defects by using Morphology Technique, *Morphology Technique International Journal of Electronics and Communication Engineering*, Vol. 9, No. 1, 2016, pp. 63-76.

[18] Y. Hanlin, W. Jun, Automatic Detection Method of Circuit Boards Defect Based on Partition Enhanced Matching, *Information Technology Journal*, Vol.12(11), 2013, pp. 2256-2260.

[19] J. Nayaka, K. Anitha, B.D. Parameshachari, R. Banud and P. Rashmi, PCB Fault Detection Using Image Processing, *IOP Conference Series: Materials Science and Engineering*, Vol.225, 2017, pp. 1-5.

[20] S. Guan, F. Guo, A New Image Enhancement Algorithm for PCB Defect Detection, *International Conference Intelligence Science and Information Engineering (ISIE)*, 2011, pp. 454-456.

Contribution of Individual Authors to the Creation of a Scientific Article (Ghostwriting Policy)

The authors contributed in the ratio of 70 (Melnyk) to 30 (Shpek) in the present research, at all stages from the formulation of the problem to the final findings and solution.

Sources of Funding for Research Presented in a Scientific Article or Scientific Article Itself

No funding was received for conducting this study.

Conflict of Interest

The authors have no conflicts of interest to declare.